Obtaining super resolution light spot using surface plasmon assisted sharp ridge nanoaperture

Eric X. Jin and Xianfan Xu[a)]
School of Mechanical Engineering, Purdue University, West Lafayette, IN 47906

(Received 15 April 2004; accepted 13 January 2005; published online 8 March 2005)

Finite difference time domain computations is used to study surface plasmon (SP) excitation around C- and H-shaped ridge nanoapertures made in silver film. The SP enhances optical transmission, in addition to the transmission mechanism of the waveguide propagation mode and Fabry-Pérot-like resonance. However, the near-field collimation of ridge aperture is found completely destroyed. On the other hand, using a bowtie-shaped aperture with sharp ridges made in silver, the loss of near-field collimation can be recovered. A super resolution optical spot with full width half magnitude as small as 12 nm$\times$16 nm is achieved due to the resonant SP excitation localized at the tips of bowtie. Much higher field enhancement is also obtained compared to the bowtie aperture made in chromium.
 [DOI: 10.1063/1.1875747]

Recently, many efforts have been made to improve transmission efficiency through subwavelength apertures and obtain sub-diffraction-limited light spots. A small circular or square aperture suffers from low throughput[1] due to waveguide cutoff. By surrounding a circular aperture with a periodic structure,[2] the emerging light can be enhanced and beamed rather than diffracted, benefiting from the interference of a composite diffracted evanescent wave [(CDEW) which includes a surface plasmon component at the metal-air interface].[3] However, the spatial resolution is limited by the period of the surrounding structure which is comparable to the wavelength.[2] Recent computational studies show that both transmission enhancement and smaller spatial resolution can be achieved using C-,[4–8] I-,[9] or H-,[8] and bowtie[8–10] shaped ridge apertures. The collimation of transmitted light through a C-shaped aperture has been confirmed by the near field optical microscopy (NSOM) measurement.[11] The ridge aperture adopts the concept of ridge waveguide in microwave engineering, and has two common features: (1) open arms which provides longer cutoff wavelength therefore allows light propagating through the aperture and (2) a narrow gap which collimates the transmitted light to a nanometer scale region. The high cutoff wavelength enables ridge nanoapertures to achieve nanoscale resolution using readily available infrared, visible, and ultraviolet laser sources, allowing many promising applications in NSOM imaging, nanolithography or nanopatterning, ultrahigh density optical data storage and thermal-assisted magnetic recording.

The transmission enhancement through a properly designed[6] ridge aperture is associated with the TE_{10} waveguide propagation mode,[4–8] and the Fabry-Pérot-like waveguide resonance[8,12,13] enhances the transmission further. In this letter, we conduct finite difference time domain (FDTD) computations to show that surface plasmon (SP) excited around C- and H-shaped ridge apertures in a silver film can provide even higher transmission, but the ridge apertures lose the near-field collimation function completely. On the other hand, for a bowtie aperture in silver, we find that a collimated near-field spot can be obtained in the event of resonant SP excitation by calculating its spectrum response at visible wavelengths. The resonant SP is a localized mode only confined at the tips of bowtie, which contributes to both the near-field collimation and extreme high field intensity. As a comparison, the bowtie aperture made in a chromium film shows a relative lower but still intense field intensity due to the lightening rod effect instead of SP excitation.

First, we consider an H-shaped aperture in a metal film deposited on a quartz substrate (dielectric constant = 2.25) with the geometry shown in the inset of Fig. 1(a). Chromium and silver are compared to show the effect of SP. The *y*-polarized illumination at 436 nm from substrate side is employed since the transmission through H-shaped aperture with *x*-polarized illumination is low and no near-field collimation exhibits.[8] The experimental data (at visible wavelengths) of complex dielectric constants of chromium[14] and silver[15] are approximated using the Drude model.[16,17] FDTD[17] calculations are conducted to show the near-field distributions inside and in the vicinity of the aperture by solving the Maxwell's equations of the differential form with a $2\times2\times2$ spatial resolution. The thickness of metal film is chosen to be 84 nm in order to maximize the transmission due to the Fabry-Pérot-like resonance effect.[8,12,13] It is also much larger than the skin depth so that the background light transmitted through the film is suppressed.

Similar calculations on H-shaped apertures can be found from earlier work,[8] but the emphasis here is to analyze the electric field component and the effect of SP. In Figs. 1(a) and 1(b), we plot *y* and *z* components of the electric field in the gap region of the chromium aperture on the *yz* plane at $x=0$. We see that the field in the gap region is dominated by the *y* component as expected. The *y*-polarized incident electric field is efficiently coupled into the aperture and well constrained between the ridges, showing the characteristics of the TE_{10} mode. On the other hand, it is seen from Fig. 1(b) that the field has a comparable *z* component on both the entrance and exit planes of the aperture. Computations show that similar field pattern of the *z* component can also be found on the aperture in a perfect conductor, indicating that this *z* component pattern partly results from scattering at the aperture edges.[3] Later we will show that SP excitation contributes to much higher field strength around the edges of the aperture in a silver film. The field distribution in Fig. 1 can

[a)]Electronic mail: xxu@ecn.purdue.edu

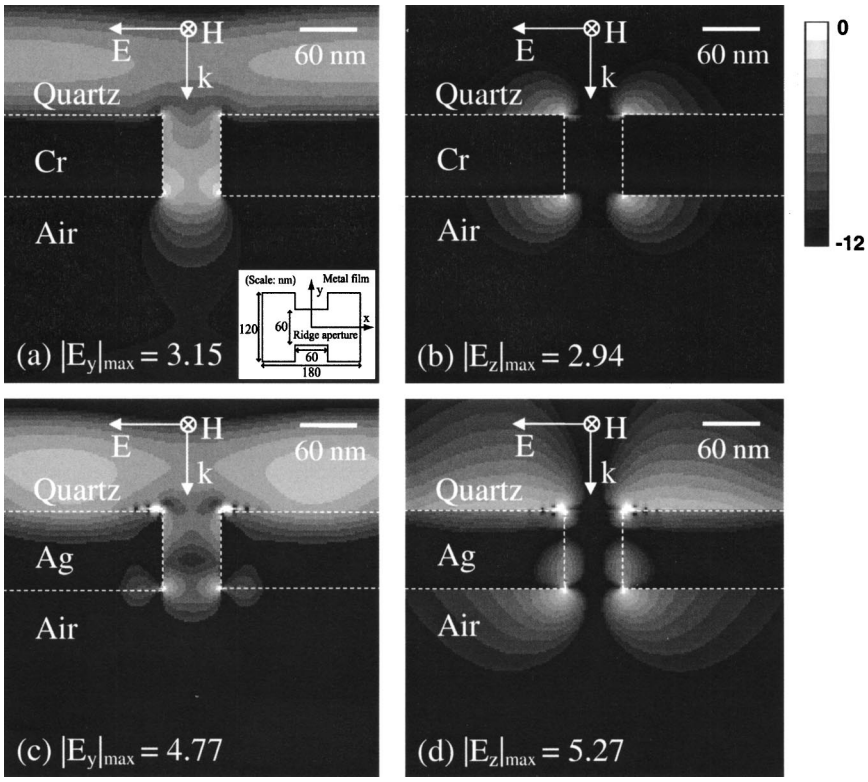

FIG. 1. Decibel scale near-field distribution of electric field strength of (a) *y* component and (b) *z* component through the H-shaped ridge aperture in chromium film, and (c) *y* component and (d) *z* component in silver film on the *yz* plane at $x=0$. The inset of (a) shows the geometry of the ridge aperture. *Y*-polarized illumination at 436 nm is normally incident from substrate side with electric field strength of unity in air.

also be understood by analyzing the aperture response to the light. Surface current is induced on the ridges by the incident photons at the entrance side, flows along the walls of the gap, and reaches the exit side. When terminated by the gap, the surface current deposits electric charges at the two ridge edges on both entrance and exit planes. The charges oscillate periodically in time and give the radiation field beyond the aperture together with the TE_{10} waveguide mode. Since the *z* field component has similar field strength compared to that of the waveguide mode at the exit plane and decays transversely, the output near-field spot is broadened slightly.

The field patterns of *y* and *z* components in a silver aperture are shown in Figs. 1(c) and 1(d), respectively. The field strength of both the *y* and *z* components is found much higher at the edges than those in the gap region, and the peak field intensity at the ridge corners in silver can reach more than 400 times of the incident field as compared to less than 36 times in chromium. The strong field strength/intensity is associated with the SP excitation due to the facts that the bulk plasma frequency of silver is in the visible range and the ratio of real to imaginary parts of the dielectric constant of silver has a large value at the excitation wavelength.[18] In addition, the field pattern on the entrance plane (the quartz–silver interface) in Fig. 2(a) clearly shows SP excitation around the aperture. Similar to the local excitation of SP around a subwavelength protrusion on silver film,[18,19] here the SP is generated by scattering from the rims of the aperture (a topological defect on flat surface).

Figures 1(c) and 1(d) also show that the SP moves into the aperture along the walls of the gap, in the same direction as the TE_{10} waveguide mode. When the propagating mode and SP reach the exit plane of the aperture, the excitation of SP occurs at the exit side around the aperture, indicated by the strong field strength. The total transmission through the aperture is therefore enhanced. This is quite different from the transmission mechanism in an array of subwavelength holes in silver, which is induced by the tunneling effect through the subwavelength holes and interference of CDEWs[3] or SPs[20–22] in the periodic structures. In an H-shaped aperture, both the waveguide mode and SP excitation provide the transmission enhancement. However, the H-shaped aperture loses its near-field collimation function completely as the transmitted light spreads around the aperture instead of focusing within the gap due to the excited SP as shown in Fig. 2(b). From our calculations, this happens to a C-shaped aperture as well (not shown here).

Also evaluated is the effect of SP on field enhancement and near-field collimation in a bowtie aperture. The bowtie aperture to be considered has a 90° bow angle and a narrow gap of $4\ \text{nm}\times 4\ \text{nm}$ [see the inset of Fig. 3(a)] in a 60-nm-thick silver film. Fine grids of $1\ \text{nm}\times 1\ \text{nm}\times 1\ \text{nm}$ are employed in the FDTD calculations to represent an accurate bowtie shape. An incident pulse containing frequency components in the visible range is used to determine the spectral response of the bowtie aperture by calculating the normalized Fourier transform of a probe field at the bowtie apex. Steady-state calculations are then conducted with a

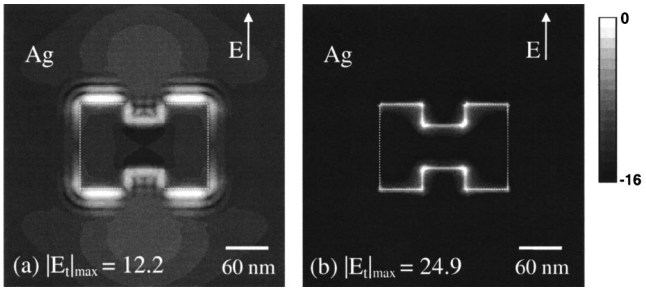

FIG. 2. Decibel scale near-field distribution in the vicinity of the H-shaped ridge aperture in silver at (a) entrance plane (silver–quartz interface) and (b) exit plane (silver–air interface). The incident electric field is *y* polarized with strength of unity in air.

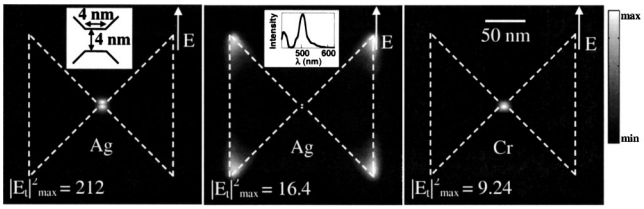

FIG. 3. Normalized field intensity ($|E_t|^2/|E_0|^2$) distribution at a distance 5 nm below a bowtie aperture in (a) 60 nm silver film with 505 nm excitation, (b) 60 nm silver film with 462 nm excitation; and (c) 60 nm chromium film with 436 nm excitation. The insets show (a) the geometry of the bowtie tips and (b) the spectrum response of the bowtie aperture in silver.

single plane wave illumination at 505 and 462 nm, respectively [a peak and a valley in the spectrum response curve as shown in the inset of Fig. 3(b)] to illustrate the bowtie aperture performance at these two wavelengths, i.e., resonance versus off-resonance.

At the 505 nm resonance, the field intensity at the bowtie apex is found more than 15,000 times that of illumination field. A near-field optical spot [full width at half maximum (FWHM) of intensity] as small as 12 nm$\times$16 nm is achieved at 5 nm below the aperture, and the peak intensity is 212 times the incident intensity as shown in Fig. 3(a). The highly confined *E* field and the extreme high field intensity, which is a result of the resonant SP excitation, depends on the geometry and dielectric constants of metal and adjacent medium.[19,23] For example, the Frohlich SP resonance for a spherical nanoparticle occurs when $\varepsilon'/\varepsilon_m=-2$ (where ε' is the real part of dielectric constant of metal, and ε_m is the dielectric constant of adjacent medium) is satisfied.[23] For the bowtie aperture in silver, SP resonance occurs at $\lambda=505$ nm, where $\varepsilon'/\varepsilon_m=-8.8$. This SP resonance condition can be understood by treating each ridge of the bowtie aperture as a prolate silver spheroid with axis aspect ratio of 3, which has the Frohlich resonance at $\varepsilon'/\varepsilon_m=-8.3$.[23] At this resonance, SP is only localized at the tips of the bowtie (similar to the ends of the long axis of spheroid). In contrary, at 462 nm off-resonance, different SP modes are excited, which are confined at corners of bowtie aperture, and the peak near-field intensity is reduced to 16.4 times that of illumination intensity as shown in Fig. 3(b).

The bowtie aperture with the same geometry as discussed previously but made in chromium is investigated as well. Because of the large absorption and a small ratio of real to imaginary parts of dielectric constant of chromium ($\varepsilon'/\varepsilon_m=-8.8$ could not be satisfied), no sharp resonance is observed in the spectrum response of the bowtie aperture in chromium. The calculation shows that, with 436 nm illumination, a small optical spot with a size (FWHM) of 16 nm $\times$14 nm and peak intensity of about 9.24 times that of incidence is obtained at 5 nm below the aperture [shown in Fig. 3(c)]. Sine SP is very weak in chromium (see the results of the H apertures), the field enhancement is not as high as in silver, and is a combined result of the waveguide propagation mode and the lightning rod or tip effect.[24]

In summary, it has been explained that in addition to the waveguide mode and Fabry-Pérot-like resonance transmission mechanisms, SP can also contribute to the transmission enhancement in a ridge aperture in silver, but has a negative effect on the near-field collimation for C- and H-shaped apertures. A bowtie aperture with sharp ridges would be a better choice to achieve higher optical resolution. Benefiting from the tip effect, a bowtie aperture in chromium has been demonstrated to provide an optical spot with FWHM as small as 16 nm$\times$14 nm. The bowtie aperture in silver provides comparable spot size but higher field intensity due to the resonant excitation of SP at the sharp tips, which recovers the loss of near-field collimation caused by the spreading of SP around C and H apertures.

Support of this work by the National Science Foundation is gratefully acknowledged.

[1] H. A. Bethe, Phys. Rev. **66**, 163 (1944).
[2] H. J. Lezec, A. Degiron, E. Devaux, R. A. Linke, L. Martin-Moreno, F. J. Garcia-vidal, and T. W. Ebbesen, Science **107**, 820 (2002).
[3] H. J. Lezec and T. Thio, Opt. Express **12**, 3629 (2004).
[4] X. Shi and L. Hesselink, Jpn. J. Appl. Phys., Part 1 **41**, 1632 (2002).
[5] X. Shi, L. Hesselink, and R. L. Thornton, Opt. Lett. **28**, 1320 (2003).
[6] X. Shi and L. Hesselink, J. Opt. Soc. Am. B **21**, 1305 (2004).
[7] A. V. Itagi, D. D. Stancil, J. A. Bain, and T. E. Schlesinger, Appl. Phys. Lett. **83**, 4474 (2003).
[8] E. X. Jin and X. Xu, Jpn. J. Appl. Phys., Part 1 **43**, 407 (2004).
[9] K. Tanaka and M. Tanaka, J. Microsc. **210**, 294 (2002).
[10] K. Sendur and W. Challener, J. Microsc. **210**, 279 (2002).
[11] F. Chen, A. Itagi, J. A. Bain, D. D. Stancil, T. E. Schlesinger, L. Stebounova, G. C. Walker, and B. B. Akhremitchev, Appl. Phys. Lett. **83**, 3245 (2003).
[12] S. Astilean, Ph. Lalanne, and M. Palamaru, Opt. Commun. **175**, 265 (2000).
[13] Y. Takakura, Phys. Rev. Lett. **86**, 5601 (2001).
[14] D. R. Lide, *CRC Handbook of Chemistry and Physics* (CRC Press, Boca Raton, FL, 1996).
[15] E. D. Palik, *Handbook of Optical Constants of Solids* (Academic, Orlando, FL, 1985).
[16] F Wooten, *Optical Properties of Solids* (Academic, New York, 1972).
[17] K. Kunz and R. Luebbers, *The Finite Difference Time Domain Method for Electromagnetics* (CRC Press, Boca Raton, FL, 1996).
[18] H. Raether, *Surface Plasmons on Smooth and Rough Surfaces and on Gratings* (Springer, Berlin, 1988).
[19] H. Ditlbacher, J. R. Krenn, N. Felidj, B. Lamprecht, G. Schider, M. Salerno, A. Leitner, and F. R. Aussenegg, Appl. Phys. Lett. **80**, 404 (2002).
[20] T. W. Ebbesen, H. J. Lezec, H. F. Ghaemi, and T. Thio, P. A. Wolff, Nature (London) **391**, 667 (1998).
[21] D. E. Grupp, H. J. Lezec, T. W. Ebbesen, K. M. Pellerin, and T. Thio, Appl. Phys. Lett. **77**, 1569 (2000).
[22] W. L. Barnes, A. Dereux, and T. W. Ebbesen, Nature (London) **424**, 824 (2003).
[23] C. F. Bohren and D. R. Huffman, *Absorption and Scattering of Light by Small Particles* (Wiley, New York, 1983).
[24] J. P. Kottmann, O. J. F. Martin, D. R. Smith, and S. Schultz, Opt. Express **6**, 213 (2000).